Title	Study of $e^+e^- \to \Upsilon(1S,2S)\eta$ and $e^+e^- \to \Upsilon(1S)\eta'$ at $\sqrt{s}$ = 10.866 GeV with the Belle detector
Author(s)	Kovalenko E., Tanida Kiyoshi, Belle Collaboration, 181 of others
Citation	Physical Review D, 104(11), p.112006_1-112006_12
Text Version	Published Journal Article
URL	https://jopss.jaea.go.jp/search/servlet/search?5074161
DOI	https://doi.org/10.1103/PhysRevD.104.112006
Right	Published by the American Physical Society under the terms of the Creative Commons Attribution 4.0 International license. Further distribution of this work must maintain attribution to the author(s) and the published article's title, journal citation, and DOI. Funded by SCOAP³.

Study of $e^+e^- \to \Upsilon(1S, 2S)\eta$ and $e^+e^- \to \Upsilon(1S)\eta'$ at $\sqrt{s} = 10.866$ GeV with the Belle detector

E. Kovalenko,[4,62] A. Garmash,[4,62] P. Krokovny,[4,62] I. Adachi,[18,14] H. Aihara,[83] D. M. Asner,[3] V. Aulchenko,[4,62] T. Aushev,[20] R. Ayad,[77] V. Babu,[8] S. Bahinipati,[24] P. Behera,[26] J. Bennett,[50] M. Bessner,[17] T. Bilka,[5] J. Biswal,[34] A. Bobrov,[4,62] A. Bondar,[4,62] G. Bonvicini,[87] A. Bozek,[59] M. Bračko,[47,34] T. E. Browder,[17] M. Campajola,[31,55] L. Cao,[2] D. Červenkov,[5] M.-C. Chang,[9] B. G. Cheon,[16] K. Chilikin,[42] H. E. Cho,[16] K. Cho,[37] S.-J. Cho,[89] S.-K. Choi,[15] Y. Choi,[75] S. Choudhury,[25] D. Cinabro,[87] S. Cunliffe,[8] S. Das,[46] G. De Nardo,[31,55] F. Di Capua,[31,55] Z. Doležal,[5] T. V. Dong,[10] S. Eidelman,[4,62,42] D. Epifanov,[4,62] T. Ferber,[8] A. Frey,[13] B. G. Fulsom,[64] R. Garg,[65] V. Gaur,[86] N. Gabyshev,[4,62] A. Giri,[25] P. Goldenzweig,[35] D. Greenwald,[79] K. Gudkova,[4,62] C. Hadjivasiliou,[64] T. Hara,[18,14] K. Hayasaka,[61] W.-S. Hou,[58] C.-L. Hsu,[76] T. Iijima,[54,53] K. Inami,[53] A. Ishikawa,[18,14] R. Itoh,[18,14] M. Iwasaki,[63] W. W. Jacobs,[27] Y. Jin,[83] K. K. Joo,[6] G. Karyan,[8] H. Kichimi,[18] C. Kiesling,[48] C. H. Kim,[16] D. Y. Kim,[74] K.-H. Kim,[89] S. H. Kim,[72] Y.-K. Kim,[89] K. Kinoshita,[7] P. Kodyš,[5] T. Konno,[36] A. Korobov,[4,62] S. Korpar,[47,34] P. Križan,[43,34] R. Kroeger,[50] T. Kuhr,[44] M. Kumar,[46] R. Kumar,[68] K. Kumara,[87] A. Kuzmin,[4,62] Y.-J. Kwon,[89] K. Lalwani,[46] J. S. Lange,[11] S. C. Lee,[40] Y. B. Li,[66] L. Li Gioi,[48] J. Libby,[26] K. Lieret,[44] D. Liventsev,[87,18] C. MacQueen,[49] M. Masuda,[82,69] T. Matsuda,[51] D. Matvienko,[4,62,42] M. Merola,[31,55] F. Metzner,[35] K. Miyabayashi,[56] R. Mizuk,[42,20] G. B. Mohanty,[78] M. Nakao,[18,14] A. Natochii,[17] L. Nayak,[25] M. Niiyama,[39] N. K. Nisar,[3] S. Nishida,[18,14] K. Ogawa,[61] S. Ogawa,[80] H. Ono,[60,61] P. Oskin,[42] P. Pakhlov,[42,52] G. Pakhlova,[20,42] S. Pardi,[31] H. Park,[40] S.-H. Park,[18] S. Patra,[23] S. Paul,[79,48] T. K. Pedlar,[45] R. Pestotnik,[34] L. E. Piilonen,[86] T. Podobnik,[43,34] E. Prencipe,[21] M. T. Prim,[2] A. Rabusov,[79] M. Röhrken,[8] A. Rostomyan,[8] N. Rout,[26] G. Russo,[55] D. Sahoo,[78] Y. Sakai,[18,14] S. Sandilya,[25] A. Sangal,[7] T. Sanuki,[81] V. Savinov,[67] G. Schnell,[1,22] C. Schwanda,[29] Y. Seino,[61] K. Senyo,[88] M. E. Sevior,[49] C. Sharma,[46] J.-G. Shiu,[58] B. Shwartz,[4,62] A. Sokolov,[30] E. Solovieva,[42] M. Starič,[34] Z. S. Stottler,[86] M. Sumihama,[12] T. Sumiyoshi,[85] W. Sutcliffe,[2] M. Takizawa,[73,19,70] U. Tamponi,[32] K. Tanida,[33] F. Tenchini,[8] K. Trabelsi,[41] M. Uchida,[84] T. Uglov,[42,20] Y. Unno,[16] K. Uno,[61] S. Uno,[18,14] P. Urquijo,[49] Y. Usov,[4,62] R. Van Tonder,[2] G. Varner,[17] A. Vinokurova,[4,62] E. Waheed,[18] C. H. Wang,[57] M.-Z. Wang,[58] P. Wang,[28] M. Watanabe,[61] O. Werbycka,[59] E. Won,[38] W. Yan,[71] S. B. Yang,[38] H. Ye,[8] J. H. Yin,[38] Y. Yusa,[61] Z. P. Zhang,[71] V. Zhilich,[4,62] and V. Zhukova[42]

(Belle Collaboration)

[1]*Department of Physics, University of the Basque Country UPV/EHU, 48080 Bilbao*
[2]*University of Bonn, 53115 Bonn*
[3]*Brookhaven National Laboratory, Upton, New York 11973*
[4]*Budker Institute of Nuclear Physics SB RAS, Novosibirsk 630090*
[5]*Faculty of Mathematics and Physics, Charles University, 121 16 Prague*
[6]*Chonnam National University, Gwangju 61186*
[7]*University of Cincinnati, Cincinnati, Ohio 45221*
[8]*Deutsches Elektronen–Synchrotron, 22607 Hamburg*
[9]*Department of Physics, Fu Jen Catholic University, Taipei 24205*
[10]*Key Laboratory of Nuclear Physics and Ion-beam Application (MOE) and Institute of Modern Physics, Fudan University, Shanghai 200443*
[11]*Justus-Liebig-Universität Gießen, 35392 Gießen*
[12]*Gifu University, Gifu 501-1193*
[13]*II. Physikalisches Institut, Georg-August-Universität Göttingen, 37073 Göttingen*
[14]*SOKENDAI (The Graduate University for Advanced Studies), Hayama 240-0193*
[15]*Gyeongsang National University, Jinju 52828*
[16]*Department of Physics and Institute of Natural Sciences, Hanyang University, Seoul 04763*
[17]*University of Hawaii, Honolulu, Hawaii 96822*
[18]*High Energy Accelerator Research Organization (KEK), Tsukuba 305-0801*
[19]*J-PARC Branch, KEK Theory Center, High Energy Accelerator Research Organization (KEK), Tsukuba 305-0801*
[20]*National Research University Higher School of Economics, Moscow 101000*
[21]*Forschungszentrum Jülich, 52425 Jülich*
[22]*IKERBASQUE, Basque Foundation for Science, 48013 Bilbao*
[23]*Indian Institute of Science Education and Research Mohali, SAS Nagar, 140306*
[24]*Indian Institute of Technology, Bhubaneswar, Satya Nagar 751007*
[25]*Indian Institute of Technology, Hyderabad, Telangana 502285*

[26]*Indian Institute of Technology, Madras, Chennai 600036*
[27]*Indiana University, Bloomington, Indiana 47408*
[28]*Institute of High Energy Physics, Chinese Academy of Sciences, Beijing 100049*
[29]*Institute of High Energy Physics, Vienna 1050*
[30]*Institute for High Energy Physics, Protvino 142281*
[31]*INFN–Sezione di Napoli, 80126 Napoli*
[32]*INFN–Sezione di Torino, 10125 Torino*
[33]*Advanced Science Research Center, Japan Atomic Energy Agency, Naka 319-1195*
[34]*J. Stefan Institute, 1000 Ljubljana*
[35]*Institut für Experimentelle Teilchenphysik, Karlsruher Institut für Technologie, 76131 Karlsruhe*
[36]*Kitasato University, Sagamihara 252-0373*
[37]*Korea Institute of Science and Technology Information, Daejeon 34141*
[38]*Korea University, Seoul 02841*
[39]*Kyoto Sangyo University, Kyoto 603-8555*
[40]*Kyungpook National University, Daegu 41566*
[41]*Université Paris-Saclay, CNRS/IN2P3, IJCLab, 91405 Orsay*
[42]*P.N. Lebedev Physical Institute of the Russian Academy of Sciences, Moscow 119991*
[43]*Faculty of Mathematics and Physics, University of Ljubljana, 1000 Ljubljana*
[44]*Ludwig Maximilians University, 80539 Munich*
[45]*Luther College, Decorah, Iowa 52101*
[46]*Malaviya National Institute of Technology Jaipur, Jaipur 302017*
[47]*Faculty of Chemistry and Chemical Engineering, University of Maribor, 2000 Maribor*
[48]*Max-Planck-Institut für Physik, 80805 München*
[49]*School of Physics, University of Melbourne, Victoria 3010*
[50]*University of Mississippi, University, Mississippi 38677*
[51]*University of Miyazaki, Miyazaki 889-2192*
[52]*Moscow Physical Engineering Institute, Moscow 115409*
[53]*Graduate School of Science, Nagoya University, Nagoya 464-8602*
[54]*Kobayashi-Maskawa Institute, Nagoya University, Nagoya 464-8602*
[55]*Università di Napoli Federico II, 80126 Napoli*
[56]*Nara Women's University, Nara 630-8506*
[57]*National United University, Miao Li 36003*
[58]*Department of Physics, National Taiwan University, Taipei 10617*
[59]*H. Niewodniczanski Institute of Nuclear Physics, Krakow 31-342*
[60]*Nippon Dental University, Niigata 951-8580*
[61]*Niigata University, Niigata 950-2181*
[62]*Novosibirsk State University, Novosibirsk 630090*
[63]*Osaka City University, Osaka 558-8585*
[64]*Pacific Northwest National Laboratory, Richland, Washington 99352*
[65]*Panjab University, Chandigarh 160014*
[66]*Peking University, Beijing 100871*
[67]*University of Pittsburgh, Pittsburgh, Pennsylvania 15260*
[68]*Punjab Agricultural University, Ludhiana 141004*
[69]*Research Center for Nuclear Physics, Osaka University, Osaka 567-0047*
[70]*Meson Science Laboratory, Cluster for Pioneering Research, RIKEN, Saitama 351-0198*
[71]*Department of Modern Physics and State Key Laboratory of Particle Detection and Electronics, University of Science and Technology of China, Hefei 230026*
[72]*Seoul National University, Seoul 08826*
[73]*Showa Pharmaceutical University, Tokyo 194-8543*
[74]*Soongsil University, Seoul 06978*
[75]*Sungkyunkwan University, Suwon 16419*
[76]*School of Physics, University of Sydney, New South Wales 2006*
[77]*Department of Physics, Faculty of Science, University of Tabuk, Tabuk 71451*
[78]*Tata Institute of Fundamental Research, Mumbai 400005*
[79]*Department of Physics, Technische Universität München, 85748 Garching*
[80]*Toho University, Funabashi 274-8510*
[81]*Department of Physics, Tohoku University, Sendai 980-8578*
[82]*Earthquake Research Institute, University of Tokyo, Tokyo 113-0032*
[83]*Department of Physics, University of Tokyo, Tokyo 113-0033*
[84]*Tokyo Institute of Technology, Tokyo 152-8550*

[85]*Tokyo Metropolitan University, Tokyo 192-0397*
[86]*Virginia Polytechnic Institute and State University, Blacksburg, Virginia 24061*
[87]*Wayne State University, Detroit, Michigan 48202*
[88]*Yamagata University, Yamagata 990-8560*
[89]*Yonsei University, Seoul 03722*

(Received 11 August 2021; accepted 12 November 2021; published 15 December 2021)

We report the first observation of the processes $e^+e^- \to \Upsilon(1S, 2S)\eta$ at $\sqrt{s} = 10.866$ GeV, with significance exceeding 10σ for both processes. The measured Born cross sections are $\sigma(e^+e^- \to \Upsilon(2S)\eta) = 2.07 \pm 0.21 \pm 0.19$ pb, and $\sigma(e^+e^- \to \Upsilon(1S)\eta) = 0.42 \pm 0.08 \pm 0.04$ pb. We also set the upper limit on the cross section of the process $e^+e^- \to \Upsilon(1S)\eta'$ to be $\sigma(e^+e^- \to \Upsilon(1S)\eta') < 0.037$ pb at 90% C.L. The results are obtained with the data sample collected with the Belle detector at the KEKB asymmetric-energy e^+e^- collider in the energy range from 10.63 to 11.02 GeV.

DOI: 10.1103/PhysRevD.104.112006

I. INTRODUCTION

Bottomonium states (bound states of $b\bar{b}$) above the $B\bar{B}$ threshold have unexpected properties. For example, the $\Upsilon(10860)$ resonance, commonly denoted as $\Upsilon(5S)$, decays into $\Upsilon(nS)\pi^+\pi^-$ ($n = 1, 2, 3$) with widths around 300–400 keV, about 2 orders of magnitude larger than those for similar decays of the $\Upsilon(2S) - \Upsilon(4S)$ which have widths around 0.5–5 keV [1]. One possible interpretation of such behavior is the existence of a light-flavor admixture in the $\Upsilon(5S)$ resonance [2,3].

Observation by the Belle collaboration of unexpectedly large values for the ratios $\frac{\Gamma(\Upsilon(5S)\to h_b(1P)\pi^+\pi^-)}{\Gamma(\Upsilon(5S)\to\Upsilon(1S)\pi^+\pi^-)} = 0.46 \pm 0.08^{+0.07}_{-0.12}$ and $\frac{\Gamma(\Upsilon(5S)\to h_b(2P)\pi^+\pi^-)}{\Gamma(\Upsilon(5S)\to\Upsilon(2S)\pi^+\pi^-)} = 0.77 \pm 0.08^{+0.22}_{-0.17}$ [4], predicted to be $\mathcal{O}(10^{-2})$ due to heavy quark spin flip [5], led to discovery of the exotic four-quark bound states, $Z_b(10610)$ and $Z_b(10650)$ [6]. A similar ratio, $\frac{\Gamma(\Upsilon(4S,5S)\to\Upsilon(1S)\eta)}{\Gamma(\Upsilon(4S,5S)\to\Upsilon(1S)\pi^+\pi^-)}$, is also expected to be $\mathcal{O}(10^{-2})$ in the QCDME model [7] but has been measured to be $2.41 \pm 0.40 \pm 0.12$ for the $\Upsilon(4S)$ [8]. Moreover, the measurement of $\mathcal{B}(\Upsilon(4S) \to \eta h_b(1P)) = (2.18 \pm 0.11 \pm 0.18) \times 10^{-3}$ [9] violates naive quark-antiquark models [10] like QCDME. Nevertheless, for bottomonium states below the $B\bar{B}$ threshold, the QCDME model predictions are consistent with measurements: $\frac{\Gamma(\Upsilon(2S)\to\Upsilon(1S)\eta)}{\Gamma(\Upsilon(2S)\to\Upsilon(1S)\pi^+\pi^-)} = (1.64 \pm 0.25) \times 10^{-3}$ [1] and $\frac{\Gamma(\Upsilon(3S)\to\Upsilon(1S)\eta)}{\Gamma(\Upsilon(3S)\to\Upsilon(1S)\pi^+\pi^-)} < 2.3 \times 10^{-3}$ [11]. Therefore, analysis of similar processes will be crucial for a better understanding of the quark structure of bottomonium states above the $B\bar{B}$ threshold.

This paper describes the study of hadronic transitions between bottomonium states with emission of an $\eta^{(\prime)}$ meson at $\sqrt{s} = 10.866$ GeV. The process $e^+e^- \to \Upsilon(2S)\eta$ is studied in two different modes: the first, $\Upsilon(2S) \to \Upsilon(1S)\pi^+\pi^-$, $\Upsilon(1S) \to \mu^+\mu^-$, $\eta \to \gamma\gamma$, denoted as $\Upsilon(2S)\eta[\gamma\gamma]$ and the second, $\Upsilon(2S) \to \mu^+\mu^-$, $\eta \to \pi^+\pi^-\pi^0$, $\pi^0 \to \gamma\gamma$, denoted as $\Upsilon(2S)\eta[3\pi]$. The process $e^+e^- \to \Upsilon(1S)\eta$ is studied in the decay chain $\Upsilon(1S) \to \mu^+\mu^-$, $\eta \to \pi^+\pi^-\pi^0$, $\pi^0 \to \gamma\gamma$, denoted as $\Upsilon(1S)\eta[3\pi]$. The process $e^+e^- \to \Upsilon(1S)\eta'$ is studied in two different modes: the first, $\Upsilon(1S) \to \mu^+\mu^-$, $\eta' \to \pi^+\pi^-\eta$, $\eta \to \gamma\gamma$, denoted as $\Upsilon(1S)\eta'[\pi\pi\eta]$ and the second, $\Upsilon(1S) \to \mu^+\mu^-$, $\eta' \to \rho^0\gamma$, $\rho^0 \to \pi^+\pi^-$, denoted as $\Upsilon(1S)\eta'[\rho\gamma]$. The $\Upsilon(1S)\eta'[\rho\gamma]$ mode is the only process with a $\mu^+\mu^-\pi^+\pi^-\gamma$ final state, while the others lead to $\mu^+\mu^-\pi^+\pi^-\gamma\gamma$ in the final state.

The first evidence for $e^+e^- \to \Upsilon(2S)\eta$ was reported in Ref. [12], measured through the recoil mass distribution against η mesons. The Born cross section [see Eq. (3)] was found to be $\sigma_B(e^+e^- \to \Upsilon(2S)\eta) = 1.02 \pm 0.30 \pm 0.17$ pb, and the upper limit $\sigma_B(e^+e^- \to \Upsilon(1S)\eta) < 0.49$ pb was set at 90% confidence limit. The results reported here are based on the reconstruction of exclusive decays and are independent of the published results.

We use a data sample of 118.3 fb^{-1} collected at the $\Upsilon(5S)$ resonance and 21 fb^{-1} collected during a scan of center-of-mass energies in the range 10.63–11.02 GeV by the Belle detector [13,14] at the KEKB asymmetric-energy e^+e^- collider [15,16]. The average center-of-mass (c.m.) energy of the $\Upsilon(5S)$ sample is $\sqrt{s} = 10.866$ GeV. The Belle detector was a large-solid-angle magnetic spectrometer that consisted of a silicon vertex detector, a 50-layer central drift chamber (CDC), an array of aerogel threshold Cherenkov counters (ACC), a barrel-like arrangement of time-of-flight scintillation counters, and an electromagnetic calorimeter comprised of CsI(Tl) crystals (ECL) located inside a superconducting solenoid coil that provided a 1.5 T magnetic field. An iron flux-return yoke located outside of

TABLE I. Selection criteria and reconstruction efficiencies, where $M^{\rm rec}_{\pi\pi} = \sqrt{s + M^2_{\pi\pi} - 2\sqrt{s}E_{\pi\pi}}$, $\delta M = M_{\mu\mu\pi\pi} - M_{\mu\mu}$, and $\Delta M_2 = M_{\Upsilon(2S)} - M_{\Upsilon(1S)} = 562$ MeV/c^2, $\Delta M_3 = M_{\Upsilon(3S)} - M_{\Upsilon(1S)} = 894$ MeV/c^2.

Criterion	$\Upsilon(2S)\eta[3\pi]$	$\Upsilon(2S)\eta[\gamma\gamma]$	$\Upsilon(1S)\eta[3\pi]$	$\Upsilon(1S)\eta'[\pi\pi\eta]$	$\Upsilon(1S)\eta'[\rho\gamma]$
$M_{\mu\mu}$ (GeV/c^2)	[9.76, 10.28]	[9.235, 9.685]	[9.235, 9.685]	[9.235, 9.685]	[9.235, 9.685]
Ψ (radian)	≥ 2	≥ 2.8	≥ 2.7	≥ 2.8	≥ 2.5
$E_{\rm tot}$ (GeV)	[10.775, 10.92]	[10.80, 10.955]	[10.75, 10.94]	[10.75, 10.94]	[10.75, 10.94]
$M_{\gamma\gamma}$ (MeV/c^2)	[110, 155]	⋯	[110, 155]	[450, 625]	⋯
δM (MeV/c^2)	⋯	$\lvert\delta M - \Delta M_2\rvert < 18$	$\lvert\delta M - \Delta M_2\rvert > 10$	$\lvert\delta M - \Delta M_2\rvert > 10$	$\lvert\delta M - \Delta M_{2,3}\rvert > 10$
$\alpha_{\pi\pi}$ (radian)	≥ 0.3	⋯	≥ 0.18	⋯	⋯
E^*_γ (MeV)	⋯	> 100	⋯	⋯	> 80
$M_{\pi\pi}$ (MeV/c^2)	⋯	⋯	⋯	⋯	[450, 950]
$M^{\rm rec}_{\pi\pi}$ (MeV/c^2)	⋯	⋯	⋯	⋯	$\lvert M^{\rm rec}_{\pi\pi} - M_{\Upsilon(2S)}\rvert > 20$
ε (%)	10.25 ± 0.03	20.73 ± 0.04	17.02 ± 0.03	13.35 ± 0.03	29.25 ± 0.05

the coil (KLM) was instrumented to detect K^0_L mesons and to identify muons.

Event selection requirements are optimized using a full Monte Carlo (MC) simulation. MC events are generated using EvtGen [17] and the detector response is modeled using GEANT3 [18]. In the simulation of $e^+e^- \to \Upsilon(1S, 2S)\eta^{(\prime)}$ we use the angular distribution dictated by the quantum numbers for a vector decay to a pseudoscalar and a vector. The dimuon decay of $\Upsilon(1S, 2S)$ is simulated to be distributed uniformly in phase space, taking into account the proper spin dynamics for decay of a massive vector meson to two leptons. For $\Upsilon(2S) \to \Upsilon(1S)\pi^+\pi^-$, we use a dipion invariant mass distribution according to the Voloshin and Zakharov model [5] measured in [19]. For the $\eta \to \pi^+\pi^-\pi^0$ decay, final state particles are distributed in phase space according to the model from [20]. Other decays are generated uniformly in phase space. Final-state radiation is taken into account using the PHOTOS package [21]. The simulation also takes into account variations of the detector configuration and beam conditions.

II. EVENT SELECTION

The event selection is performed in two steps. First we require the presence of at least two oppositely charged muon and two oppositely charged pion candidates. Charged tracks must originate from a cylindrical region within ± 2.5 cm along the z axis (opposite the positron beam) and 2 cm in the transverse direction, relative to the e^+e^- interaction point. Muon candidates are identified with a requirement on a likelihood ratio $\mathcal{P}_\mu = \frac{\mathcal{L}_\mu}{\mathcal{L}_\mu + \mathcal{L}_\pi + \mathcal{L}_K} > 0.1$ (efficiency is ≈99.9%), where the likelihood $\mathcal{L}_i$, with $i = \mu$, π, K, is assigned based on the range of the particle extrapolated from the CDC through KLM and on the deviation of hit positions from the extrapolated track [22]. Every charged particle that is not identified as a muon or an electron ($\mathcal{P}_e < 0.99$) is considered to be a charged pion, where $\mathcal{P}_e$ is a similar likelihood ratio based on CDC, ACC, and ECL information [23]. Additionally, we require the dimuon invariant mass $M_{\mu\mu}$ to satisfy 8 GeV/$c^2 < M_{\mu\mu} <$ 12 GeV/c^2 and dipion invariant mass $M_{\pi\pi} < 4$ GeV/c^2. At this stage, no requirements on photon candidates are applied.

Final-state-specific requirements are applied at the second stage. The following set of selection variables are common to all processes: the angle Ψ between the total momentum of the photons and the total momentum of the charged particles in the e^+e^- c.m. frame, the invariant mass of the muon pair $M_{\mu\mu}$ [corresponding to the $\Upsilon(1S, 2S)$], and the total reconstructed energy of the final-state particles, $E_{\rm tot}$. These variables are used to select exclusive decay chains that result in the same final states $\mu^+\mu^-\pi^+\pi^-\gamma(\gamma)$.

The signal region for $\Upsilon(1S) \to \mu^+\mu^-$ is defined to be 9.235 GeV/$c^2 < M_{\mu\mu} <$ 9.685 GeV/c^2 and that for $\Upsilon(2S) \to \mu^+\mu^-$ is 9.76 GeV/$c^2 < M_{\mu\mu} <$ 10.28 GeV/c^2. Four-momentum conservation requires the angle Ψ to be equal to π radian; however, it can deviate even for true candidates due to finite momentum and energy resolutions. For the $\Upsilon(2S)\eta[3\pi]$ mode this effect results in a less strict requirement on the angle Ψ due to the low momentum of the π^0. Selection criteria for the angle Ψ are listed in Table I for all modes. If multiple candidates occur in an event, usually due to additional photons from background processes, the $\mu\mu\pi\pi\gamma(\gamma)$ combination with Ψ closest to π radians is chosen as the best candidate. According to the simulation, the fraction of events containing multiple candidates is ≈24% for the $\Upsilon(2S)\eta[3\pi]$ mode and ranges from 3% to 12% for other modes. Finally, $E_{\rm tot}$ is calculated as

$$E_{\rm tot} = E_{\pi\pi\gamma(\gamma)} + \sqrt{M^2_{\Upsilon(1S,2S)} + \vec{P}^2_{\mu\mu}}, \qquad (1)$$

where, instead of the reconstructed value of the $\mu^+\mu^-$-pair invariant mass, the world-average mass of the Υ meson is used [1]. This approach allows one to improve the $E_{\rm tot}$ resolution by removing the contribution from the $M_{\mu\mu}$ resolution, whose value is about 50 MeV/c^2 and

comparable to the total contribution of all other terms in $E_{\rm tot}$. Selection requirements on these common variables for all considered decay chains are summarized in Table I. Additional criteria for the selection of specific modes are described below.

To reconstruct a neutral pion from the $\pi^0 \to \gamma\gamma$ decay in the $\Upsilon(1S, 2S)\eta[3\pi]$ modes, the invariant mass $M_{\gamma\gamma}$ must be in the signal range $110\ {\rm MeV}/c^2 < M_{\gamma\gamma} < 155\ {\rm MeV}/c^2$, where the resolution is $5.5\ {\rm MeV}/c^2$. For the $\Upsilon(1S)\eta'[\pi\pi\eta]$ mode the η meson is reconstructed from the $\eta \to \gamma\gamma$ decay with a signal range $450\ {\rm MeV}/c^2 < M_{\gamma\gamma} < 625\ {\rm MeV}/c^2$, where the resolution is $12.3\ {\rm MeV}/c^2$. For the $\Upsilon(1S)\eta'[\rho\gamma]$ mode the ρ^0 resonance is reconstructed from the $\rho^0 \to \pi^+\pi^-$ decay with a signal range $450\,{\rm MeV}/c^2 < M_{\pi\pi} < 950\,{\rm MeV}/c^2$.

For the two-body $\Upsilon(5S) \to \Upsilon(2S)\eta[\gamma\gamma]$ decay the η meson is monochromatic, with a c.m. momentum equal to $615\ {\rm MeV}/c$. Thus, the photons produced in a $\eta \to \gamma\gamma$ decay have an energy distributed in the range 105–715 MeV in the c.m. frame. We require the photon energy to be greater than 100 MeV, which significantly reduces combinatorial background and has virtually no effect on signal events.

For the $\Upsilon(2S)\eta[\gamma\gamma]$ final state the $\Upsilon(2S)$ meson is reconstructed via its decay chain $\Upsilon(2S) \to \Upsilon(1S)\pi^+\pi^-$ with $\Upsilon(1S) \to \mu^+\mu^-$. We calculate the mass difference $M_{\mu\mu\pi\pi} - M_{\mu\mu} = \delta M$, where the correlated contributions to resolution from the muon momentum measurement substantially cancel. The peak of δM corresponds to $\Delta M = M_{\Upsilon(2S)} - M_{\Upsilon(1S)} = 562\ {\rm MeV}/c^2$, and the resolution is approximately $4.6\ {\rm MeV}/c^2$. A requirement of $|\delta M - \Delta M| < 18\ {\rm MeV}/c^2$ is applied.

For all modes, the signal is found by fitting the $M_{\eta^{(\prime)}}$ ($M_{\gamma\gamma}$, $M_{\pi\pi\gamma\gamma}$ or $M_{\pi\pi\eta}$) invariant mass distribution, as it has no peaking background (see Sec. III). The MC signal distribution is taken as a sum of a Crystal Ball function [24] and a Gaussian. The reconstruction efficiency ε is then determined as $N_{\rm det}/N_{\rm gen}$, where $N_{\rm det}$ is the integral of the fitted function and $N_{\rm gen} = 10^6$. Results are summarized in Table I.

III. STUDY OF THE EXPECTED BACKGROUND

The most relevant background to this analysis comes from transitions between other bottomonium states with emission of an $\eta^{(\prime)}$. Such decays have an $\eta^{(\prime)}$ invariant mass distribution identical to our signal modes.

Due to the η' mass and parity considerations, the η' meson can originate only from the $\Upsilon(5S) \to \Upsilon(1S)\eta'$ decay or from $\Upsilon(5S) \to \chi_{bJ}(1P)\eta'\gamma$ decays with a subsequent radiative decay $\chi_{\rm bJ}(1P) \to \Upsilon(1S)\gamma$. The former is our signal and the latter is suppressed by the presence of an additional photon.

In contrast, the η meson can also originate from $\Upsilon(5S) \to \Upsilon(1D)\eta$ [12] and $\Upsilon(5S) \to \Upsilon(2S, 3S)X$ followed by $\Upsilon(2S, 3S) \to \Upsilon(1S)\eta$ decays. For the $\Upsilon(5S) \to \Upsilon(1D)\eta$ decay, the most relevant channels are those with $\Upsilon(1D) \to \chi_{bJ}\gamma \to \Upsilon(1S)\gamma\gamma$ and $\Upsilon(1D) \to \Upsilon(1S)\pi^+\pi^-$ decays. However, the first decay chain has two extra photons in the final state and is suppressed by the requirement on $E_{\rm tot}$. The second decay might produce a correct set of final-state particles (with $\eta \to \gamma\gamma$), but is significantly suppressed by the requirement on $M_{\mu\mu\pi\pi} - M_{\mu\mu}$: for the $\Upsilon(1D) \to \Upsilon(1S)\pi^+\pi^-$ decay, this variable peaks in δM at approximately $140\ {\rm MeV}/c^2$ higher than for the $\Upsilon(2S) \to \Upsilon(1S)\pi^+\pi^-$ with a resolution of about $5\ {\rm MeV}/c^2$. Therefore, the $\Upsilon(1D) \to \Upsilon(1S)\pi^+\pi^-$ signal fails our criteria and is completely eliminated.

The decay chain $\Upsilon(5S) \to \Upsilon(2S, 3S)\pi^+\pi^-$, $\Upsilon(2S, 3S) \to \Upsilon(1S)\eta$, $\eta \to \gamma\gamma$ produces the same set of final-state particles and the same signal distribution as the $\Upsilon(2S)\eta[\gamma\gamma]$ mode. However, the branching fractions $\mathcal{B}(\Upsilon(2S, 3S) \to \Upsilon(1S)\eta)$ are small, and with the current integrated luminosity the expected number of η mesons produced by this mechanism is estimated to be 2 for the $\Upsilon(2S)$ and less than 1 for the $\Upsilon(3S)$. Contributions from these decays are also strongly suppressed by the requirement on $M_{\mu\mu\pi\pi} - M_{\mu\mu}$; its mean value deviates from the $\Upsilon(2S) \to \Upsilon(1S)\pi^+\pi^-$ signal window by $280\ {\rm MeV}/c^2$ and $50\ {\rm MeV}/c^2$ for $\Upsilon(5S) \to \Upsilon(2S)\pi^+\pi^-$ and $\Upsilon(5S) \to \Upsilon(3S)\pi^+\pi^-$, respectively.

A possible source of background for $\Upsilon(5S) \to \Upsilon(2S)\eta$ is from the decay itself, with $\Upsilon(2S) \to \Upsilon(1S)\eta$, where $\eta \to \pi^+\pi^-\pi^0$ or $\eta \to \pi^+\pi^-\gamma$. This final state is similar to the $\Upsilon(2S)\eta[\gamma\gamma]$ mode when a soft photon or π^0 is undetected. Nevertheless, this background is negligible due to the small branching fraction, $\frac{\mathcal{B}(\Upsilon(2S)\to\Upsilon(1S)\eta)\times\mathcal{B}(\eta\to\pi^+\pi^-\pi^0(\gamma))}{\mathcal{B}(\Upsilon(2S)\to\Upsilon(1S)\pi^+\pi^-)} \sim 4\times10^{-4}$, and requirements on $E_{\rm tot}$.

Crossfeed between the signal modes is a source of background that passes the common selection criteria but does not produce peaks in the signal distributions. For the $\Upsilon(1S)\eta[3\pi]$ and $\Upsilon(1S)\eta'$ modes, there is such a background from the $\Upsilon(2S)\eta[\gamma\gamma]$ mode when $\Upsilon(2S) \to \Upsilon(1S)\pi^+\pi^-$. To reduce this background for the $\Upsilon(1S)\eta^{(\prime)}$ mode, we require $|M_{\mu\mu\pi\pi} - M_{\mu\mu} - (M_{\Upsilon(2S)} - M_{\Upsilon(1S)})| > 10\,{\rm MeV}/c^2$, which only slightly decreases the signal reconstruction efficiency and suppresses this background to a negligible level. The crossfeed between the $\Upsilon(1S)\eta[3\pi]$ and $\Upsilon(2S)\eta[3\pi]$ modes is efficiently removed by the common selection requirements.

Another significant part of the background is the non-peaking combinatorial background. To evaluate the expected level, we used a set of MC events equivalent to 6 times the integrated luminosity of the data and including the following processes: $e^+e^- \to c\bar{c}$, $u\bar{u}$, $d\bar{d}$, $s\bar{s}$; $e^+e^- \to B_s^{(*)}\bar{B}_s^{(*)}$, $B^{(*)}\bar{B}^{(*)}(\pi)$; and known decays of the $\Upsilon(5S)$. In addition, we performed a simulation of $e^+e^- \to \tau^+\tau^-$ events with statistics equivalent to the integrated

luminosity of our dataset. The only events remaining after the application of our selection criteria originate from $\Upsilon(5S)$ decays to final states containing bottomonium. For example, the dominant background to the $\Upsilon(2S)\eta[\gamma\gamma]$ comes from the $\Upsilon(2S)\pi^0\pi^0$ final state, which produces a broadly peaking $M_{\gamma\gamma}$ distribution from 50 to 850 MeV/c^2 with a maximum near the signal η peak position. To suppress this background, we tightened the requirement on the total reconstructed energy from 10.75 to 10.80 GeV for the $\Upsilon(2S)\eta[\gamma\gamma]$ mode. This reduces the expected number of background events for the $\Upsilon(2S)\eta[\gamma\gamma]$ from 20 to 5 events and slightly decreases the detection efficiency.

For the $\Upsilon(1S)\eta'[\rho\gamma]$ mode, the MC study predicts a high background from the $\Upsilon(5S) \to \Upsilon(2S)\pi^+\pi^-$ decay, where $\Upsilon(2S) \to \mu^+\mu^-\gamma(\gamma)$. To reduce this background we set a veto on the recoil mass $M^{\rm rec}_{\pi\pi}$: $|M^{\rm rec}_{\pi\pi} - M_{\Upsilon(2S)}| > 20\,{\rm MeV}/c^2$. The MC study also predicts background contributions from decays with the $\Upsilon(2S,3S) \to \Upsilon(1S)[\mu^+\mu^-]\pi^+\pi^-$ intermediate transition. Therefore, we reduced this background in the same way as for the $\Upsilon(1S)\eta[3\pi]$ and $\Upsilon(1S)\eta'[\pi\pi\eta]$ modes by setting vetoes $|M_{\mu\mu\pi\pi} - M_{\mu\mu} - (M_{\Upsilon(2S,3S)} - M_{\Upsilon(1S)})| > 10\,{\rm MeV}/c^2$. Moreover, there are no requirements on photons except the general one from four-momentum conservation, therefore we expect background from low-energy photons. To suppress this background we set a minimum photon energy in the c.m. frame of $E^*_\gamma > 80$ MeV. This requirement reduces the reconstruction efficiency by factor of 1.12, and greatly reduces background.

We find that all these sources, predicted by the background MC, account for less than 30% of the observed background in the sideband data. The remainder of the background is thought to originate from QED processes that, in general, have much higher cross sections, e.g., processes like $e^+e^- \to \mu^+\mu^-\gamma \to \mu^+\mu^-e^+e^-$. This e^+e^- pair could be reconstructed as a pair of collinear pions. A selection requirement on the opening angle between two charged pion candidates of $\alpha_{\pi\pi} > 0.18$ radian for the $\Upsilon(1S)\eta[3\pi]$ mode and of $\alpha_{\pi\pi} > 0.3$ radian for the $\Upsilon(2S)\eta[3\pi]$ mode reduces this background substantially.

Finally, we tested for possible background from nonresonant $e^+e^- \to \mu^+\mu^-\eta^{(\prime)}$ decays using experimental data with the requirement on $M_{\mu\mu}$ shifted to central values ranging from 8 to 9 GeV/c^2, i.e., lower than the ground bottomonium state. No evidence for such processes was observed.

IV. DATA ANALYSIS

A. Cross section at the $\Upsilon(5S)$ resonance

The signal yield is determined from a binned maximum likelihood fit to the invariant mass $M_{\eta^{(\prime)}}$ ($M_{\gamma\gamma}$, $M_{\pi\pi\gamma\gamma}$ or $M_{\pi\pi\gamma}$) distribution (Figs. 1 and 2), with the fitting function being the sum of the signal function and a background function $(x - p_1)^{p_2} e^{p_3 x}$, where p_1, p_2, p_3 are floating parameters. All parameters of the signal function, except its normalization factor and the Crystal Ball peak position, are fixed to the values determined from the fit to the MC distribution, with the difference in position between Crystal Ball and Gaussian peaks being fixed.

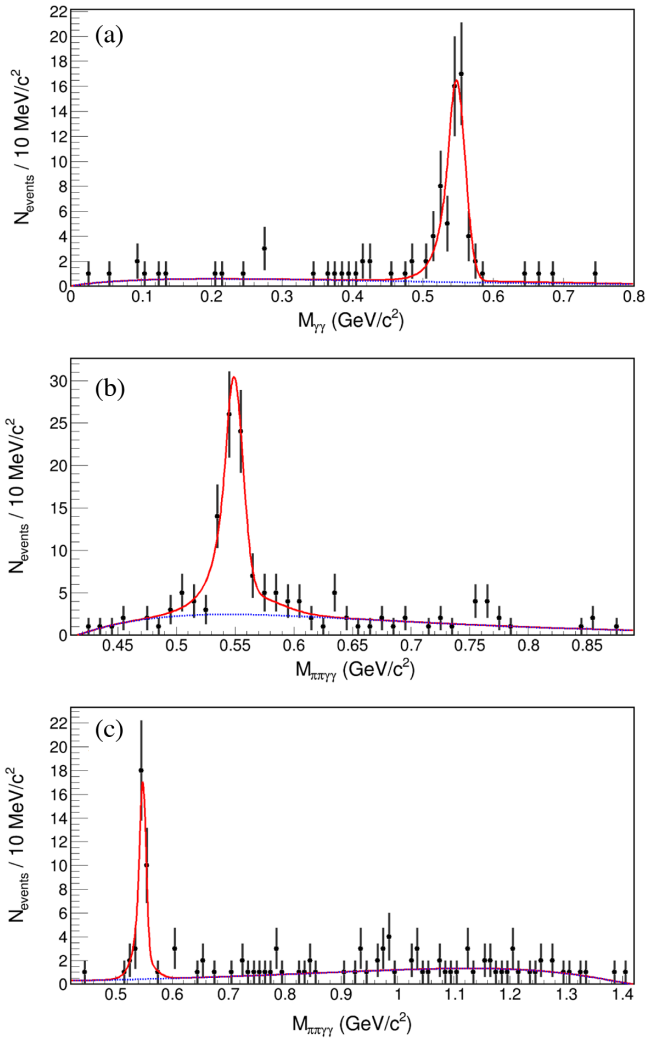

FIG. 1. The experimental signal M_η ($M_{\gamma\gamma}$ or $M_{\pi\pi\gamma\gamma}$) distribution for (a) $\Upsilon(2S)\eta[\gamma\gamma]$, (b) $\Upsilon(2S)\eta[3\pi]$, and (c) $\Upsilon(1S)\eta[3\pi]$ fitted to the sum of the MC signal function and background function $(x - p_1)^{p_2} e^{p_3 x}$. Data are shown as points, the solid red line shows the best fit to the data, and the dashed blue line shows the background contribution.

The visible cross section is

$$\sigma_{\rm vis} = \frac{N_{\rm sig}}{L\mathcal{B}\varepsilon}, \tag{2}$$

where $N_{\rm sig}$ is the fitted signal yield, L is the integrated luminosity, $\mathcal{B}$ is the product of the intermediate branching fractions for the process, and ε is the reconstruction efficiency.

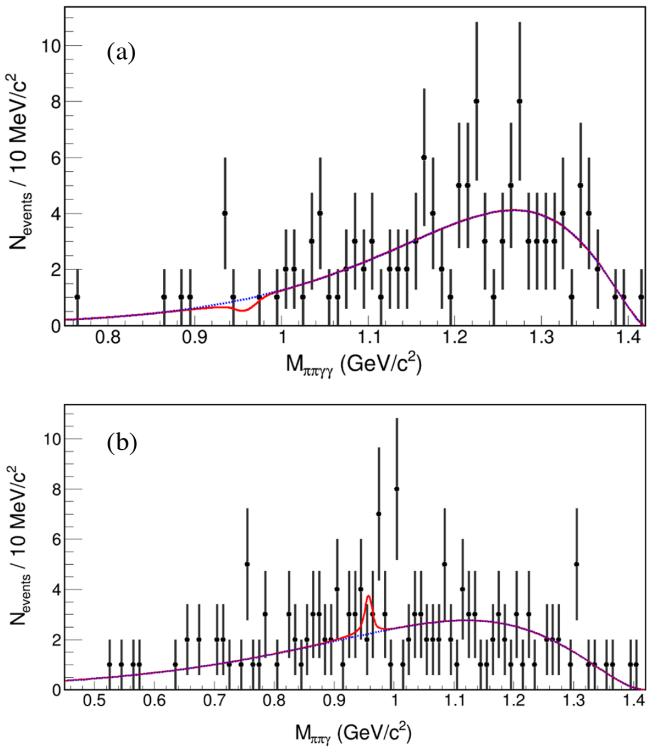

FIG. 2. The experimental signal $M_{\eta'}$ ($M_{\pi\pi\gamma\gamma}$ or $M_{\pi\pi\gamma}$) distribution for (a) $\Upsilon(1S)\eta'[\pi\pi\eta]$ and (b) $\Upsilon(1S)\eta'[\rho\gamma]$ fitted to the sum of the MC signal function and background function $(x - p_1)^{p_2} e^{p_3 x}$. Data are shown as points, the solid red line shows the best fit to the data, and the dashed blue line shows the background contribution.

For the $\Upsilon(2S)\eta[\gamma\gamma]$, $\Upsilon(2S)\eta[3\pi]$, and $\Upsilon(1S)\eta[3\pi]$ modes we evaluate the signal significance as $\sqrt{2\log[\mathcal{L}(N)/\mathcal{L}(0)]}$, where $\mathcal{L}(N)/\mathcal{L}(0)$ is the ratio between the likelihood values for a fit that includes a signal yield N and a fit with a background hypothesis only. The calculated significances are 12.8σ, 10.5σ, and 10.2σ, respectively. Thus, we report the first observation of the $e^+e^- \to \Upsilon(2S)\eta$ process in both modes and the first observation of the $e^+e^- \to \Upsilon(1S)\eta$ process at $\sqrt{s} = 10.866$ GeV. Setting the requirement $520 < M_\eta < 580$ MeV, we also confirm that there are clear peaks in $M_{\mu\mu}$ distributions (Fig. 3), consistent with $\Upsilon(1S, 2S) \to \mu^+\mu^-$, for these modes.

For the $\Upsilon(1S)\eta'[\pi\pi\eta]$ and the $\Upsilon(1S)\eta'[\rho\gamma]$ modes the signal yield is $N_{\rm sig} = -1.76 \pm 3.30$ and $N_{\rm sig} = 3.30 \pm 4.41$ respectively; upper limits are set using a pseudo-experiment method. In this method we simulate 10^5 trials, for which background number of events is distributed according to the Poisson distribution with the mean matching the number observed in the data and the signal events generated with a given signal yield. A value of $M_{\pi\pi\gamma(\gamma)}$ is generated according to the background line shape obtained from the fit to the data for each background event, and according to MC signal shape for each signal event. Then, the $M_{\pi\pi\gamma(\gamma)}$ distribution for each trial is fitted using the same procedure as with data, and the obtained signal yield is recorded. A confidence limit, C.L., is calculated from the distribution of the fit results as a fraction of events with the signal yield exceeding $N_{\rm sig}$ obtained from the fit to the data. Repeating the procedure for several generated signal yield values, 90% C.L. signal yield is obtained from *C.L. vs generated signal yield* curve. As a result, the 90% C.L. upper limits for the $\Upsilon(1S)\eta'[\pi\pi\eta]$ and $\Upsilon(1S)\eta'[\rho\gamma]$ modes are found to be $N_{\rm sig} = 2.1$ and $N_{\rm sig} = 8.3$, respectively.

Table II shows the signal yields, calculated visible cross sections, and peak positions for the η meson, which are consistent with the world-average value $M_\eta = 547.86 \pm 0.02$ MeV/c^2 [1] within the statistical uncertainty.

B. Cross section outside of $\Upsilon(5S)$

We study the cross section behavior of the processes below the $\Upsilon(5S)$ to estimate radiative corrections. For this study we use 21 fb^{-1} of data collected at c.m. energies from 10.63 to 11.02 GeV. We group these data into three energy bands: 10.63–10.77 GeV (A), 10.83–10.91 GeV (B) and 10.93–11.02 GeV (C). They are analyzed in the same way as the data on the $\Upsilon(5S)$ except for the requirement on $E_{\rm tot}$, which is shifted to the corresponding CMS energy. This analysis shows (Table III) that there are no signal events in band A except for one event in the $\Upsilon(2S)\eta[3\pi]$ and $\Upsilon(1S)\eta'[\rho\gamma]$ modes. For each mode we set upper limits $N_{\rm sig} < 1$ corresponding to a C.L. of 63%.

For the $\Upsilon(1S)\eta[3\pi]$, $\Upsilon(1S)\eta'[\pi\pi\eta]$, and $\Upsilon(1S)\eta'[\rho\gamma]$ modes, the upper limits are higher than the values measured

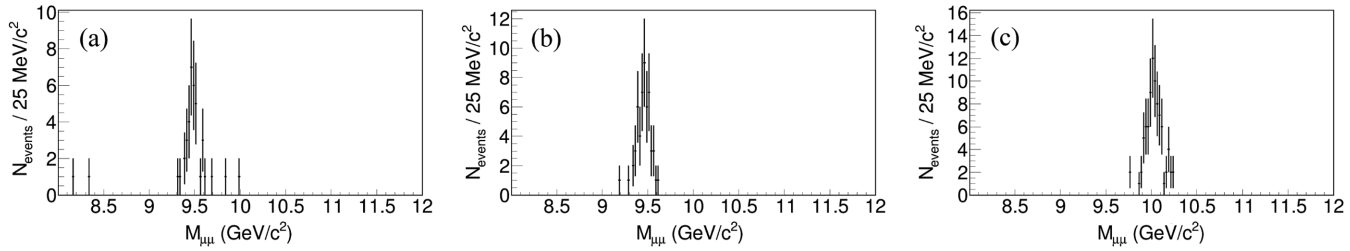

FIG. 3. The $M_{\mu\mu}$ distribution for the $\Upsilon(5S)$ data with the requirement $520 < M_\eta < 580$ MeV for (a) $\Upsilon(1S)\eta[3\pi]$, (b) $\Upsilon(2S)\eta[\gamma\gamma]$, and (c) $\Upsilon(2S)\eta[3\pi]$ modes. No requirement on $M_{\mu\mu}$ is applied.

TABLE II. Signal yield, visible cross section, and obtained $M_{\eta^{(\prime)}}$ peak position for all modes at $\sqrt{s} = 10.866$ GeV. The uncertainties are statistical only.

Mode	$N_{\rm sig}$	$\sigma_{\rm vis}$ (pb)	$M_{\eta^{(\prime)}}$ (MeV/c^2)
$\Upsilon(2S)\eta[\gamma\gamma]$	59.5 ± 8.3	1.39 ± 0.19	547.8 ± 2.0
$\Upsilon(2S)\eta[3\pi]$	73.8 ± 10.7	1.39 ± 0.20	549.1 ± 1.5
$\Upsilon(1S)\eta[3\pi]$	32.6 ± 5.9	0.29 ± 0.05	547.9 ± 1.3
$\Upsilon(1S)\eta'[\pi\pi\eta]$	< 2.1, C.L. $= 90\%$	< 0.030, C.L. $= 90\%$	...
$\Upsilon(1S)\eta'[\rho\gamma]$	< 8.3, C.L. $= 90\%$	< 0.031, C.L. $= 90\%$	...

TABLE III. Results of the scan data analysis and comparison of the averaged upper limits on cross section in band A (10.63–10.77 GeV) with results from the main dataset. $N_{\rm sig}$ is the signal yield and $N_{\rm tot}$ is the total number of events in the signal distribution.

Mode	$\sqrt{s}$ range (GeV)	L (fb^{-1})	$N_{\rm sig}$	$N_{\rm tot}$	$\sigma_{\rm vis}$ in band A (pb)	$\sigma_{\rm vis}$ at $\Upsilon(5S)$ (pb)
$\Upsilon(2S)\eta[\gamma\gamma]$	10.63–10.77	3.8	0	2	< 0.45, C.L. $= 63\%$	1.39 ± 0.14
	10.83–10.91	10.1	2.0 ± 1.5	5		
	10.93–11.02	7.1	1.0 ± 1.0	2		
$\Upsilon(2S)\eta[3\pi]$	10.63–10.77	3.8	1.0 ± 1.0	1		
	10.83–10.91	10.1	17.3 ± 4.4	21		
	10.93–11.02	7.1	0	1		
$\Upsilon(1S)\eta'[\pi\pi\eta]$	10.63–10.77	3.8	0	3	< 0.116, C.L. $= 63\%$	< 0.023, C.L. $= 90\%$
	10.83–10.91	10.1	0	8		
	10.93–11.02	7.1	0	8		
$\Upsilon(1S)\eta'[\rho\gamma]$	10.63–10.77	3.8	0.8 ± 1.2	3		
	10.83–10.91	10.1	0	18		
	10.93–11.02	7.1	1.3 ± 1.8	18		
$\Upsilon(1S)\eta[3\pi]$	10.63–10.77	3.8	0	1	< 0.27, C.L. $= 63\%$	0.29 ± 0.05
	10.83–10.91	10.1	0.9 ± 1.1	11		
	10.93–11.02	7.1	1.0 ± 1.0	3		

at the $\Upsilon(5S)$ resonance, while for the $e^+e^- \to \Upsilon(2S)\eta$ process the upper limit indicates resonance production of the final state. Since resonance production has been observed in similar processes $e^+e^- \to \Upsilon(1S, 2S, 3S)\pi^+\pi^-$ [25,26] and $e^+e^- \to h_b(1P, 2P)\pi^+\pi^-$ [27], and our new results do not rule it out, we assume a resonance model to calculate the radiative correction for all modes as described, for example, in [28], neglecting the possible energy dependence of the resonance width. For this calculation, the following $\Upsilon(5S)$ parameters are used: $M_{\Upsilon(5S)} = 10885.2$ MeV/c^2, $\Gamma_{\Upsilon(5S)} = 37$ MeV [1]. We calculate radiative correction $1 + \delta$ to vary from 0.624 to 0.628 for different modes. This correction is used to calculate the Born cross section ($\sigma_{\rm B}$) as

$$\sigma_{\rm B} = \sigma_{\rm vis} \frac{|1 - \Pi|^2}{1 + \delta}, \tag{3}$$

where $|1 - \Pi|^2 = 0.929$ is the vacuum-polarization factor [12,29].

C. Systematic uncertainties

The particle reconstruction efficiency and particle identification are important parameters whose values in simulation could differ from those in the experiment. According to independent studies, for example using the $D^{*-} \to \pi^- \bar{D}^0[K^0_S\pi^+\pi^-]$ decay, the systematic uncertainty due to track reconstruction is 1% for pions and 0.35% for high-momentum muons [30]. The photon reconstruction uncertainty is 1.5%. The muon identification uncertainty is 1%, according to analysis of $J/\psi \to \mu^+\mu^-$ [30]. Therefore, the total systematic uncertainty for the $\mu^+\mu^-\pi^+\pi^-\gamma$ and $\mu^+\mu^-\pi^+\pi^-\gamma\gamma$ final states is 2.7% from charged track reconstruction, 1.5% and 3% respectively from photon reconstruction and 2% from muon identification.

Another uncertainty can come from the accuracy of the PHOTOS module, which describes final-state radiation. To evaluate this uncertainty we simulate the $\Upsilon(2S)\eta[\gamma\gamma]$ and $\Upsilon(2S)\eta[3\pi]$ modes without the PHOTOS module. For both processes the cross section increases by 9% mostly due to the absence of radiation by muons, which could account for hundreds of MeV of energy. Thus, the total influence of PHOTOS on the efficiency is 9% while its own uncertainty is a few percent [21]; therefore, the uncertainty on the detection efficiency appears in the next order and we take 1% as a conservative estimate.

The dependence of the cross section on c.m. energy could differ from a pure Breit-Wigner. As an alternative

TABLE IV. Systematic uncertainties.

Uncertainty (%)	$\Upsilon(2S)\eta[\gamma\gamma]$	$\Upsilon(2S)\eta[3\pi]$	$\Upsilon(1S)\eta[3\pi]$	$\Upsilon(1S)\eta'[\pi\pi\eta]$	$\Upsilon(1S)\eta'[\rho\gamma]$
Track reconstruction			2.7		
Muon identification			2.0		
Luminosity L			1.4		
PHOTOS			1.0		
Radiative correction	4.3	5.1	5.7	5.7	5.7
Photon reconstruction	3.0	3.0	3.0	3.0	1.5
Intermediate branchings	2.5	8.9	2.4	2.7	2.4
Selection criteria	6.0	6.6	5.6	···	···
Resolution	2.1	1.4	1.1	···	···
Signal line shape	1.0	1.4	1.4	···	···
Background line shape	1.5	1.0	1.1	···	···
Binning	0.3	2.1	0.8	···	···
Total	9.6	13.4	9.8	10.0	9.5

dependence we add to the $\Upsilon(5S)$ Breit-Wigner a constant contribution with an amplitude derived from the upper limit of 0.45 pb found in band A (see Table III). The upper limit of 0.45 pb corresponds to 0.58 pb after applying the correction for initial-state radiation. Considering this to be a constant contribution to the Born cross section and using the visible cross section of 1.39 pb at $\sqrt{s} = 10.866$ GeV (Table II), we estimate that the corrected cross section at $\sqrt{s} = 10.866$ GeV is 2.10 pb, thus the constant component constitutes a fraction $0.58/2.10 = 0.276$. Using this cross section dependence, we calculate a radiative correction for all modes. Its deviation from the nominal values ranges from 4.3% to 5.7% and is referred to as the radiative correction uncertainty.

To estimate the influence of selection criteria we vary three unified requirements: the width of the $E_{\rm tot}$ signal range is symmetrically varied by ± 60 MeV from the nominal value, the lower boundary for the angle Ψ is varied from 2 to 2.8 radians, and the width of the $M_{\mu\mu}$ signal range is symmetrically varied by ± 200 MeV$/c^2$ from the nominal value. The maximum cross section deviation from the nominal is taken as a systematic uncertainty. The total uncertainty due to selection criteria is the quadratic sum of these three contributions and is shown in Table IV.

One more indication of systematic error is the deviation between simulated and experimental resolutions—experimental distributions are usually wider than those in simulation. To estimate the uncertainty from this source, we choose events with the $\Upsilon(1S)$ originating from $\Upsilon(2S) \to \Upsilon(1S)\pi^+\pi^-$, using the requirement $|M_{\mu\mu\pi\pi} - M_{\mu\mu} - (M_{\Upsilon(2S)} - M_{\Upsilon(1S)})| < 18$ MeV$/c^2$. Parametrization of the experimental $M_{\mu\mu}$ distribution with a sum of a Gaussian and linear function finds a resolution of 54 ± 1.5 MeV$/c^2$, which is larger than the resolution in MC of 50 MeV$/c^2$ by 8%. This deviation is common for other distributions; therefore, we vary the resolution of the signal $M_{\eta^{(\prime)}}$ distribution by $\pm 10\%$ to evaluate the reconstruction efficiency in MC and fit to the experimental data. The maximum deviation of the cross section from the nominal one is referred to as the resolution uncertainty. Additionally, we verified that the data parametrization with floating resolution is consistent with the simulation within the statistical uncertainty.

The uncertainty due to signal line shape is taken as the maximum difference of the cross section between data fits with different signal parametrizations. The nominal line shape is the sum of the Crystal Ball function and a Gaussian, while two tested alternate line shapes are a Gaussian only and a Crystal Ball only. The uncertainty due to background line shape is the maximum difference of the cross section between fits to the data in different signal ranges—in this way not every background event is included in the fit and the background line shape changes.

The $\eta' \to \pi^+\pi^-\eta$ decay was simulated uniformly in phase space, which is not necessarily the correct representation of dynamics of this process. However, Ref. [31] shows that experimental Dalitz distributions are consistent with a uniform distribution over phase space; thus, this source of uncertainty is neglected.

The bin width of the fitted distribution in $M_{\eta^{(\prime)}}$ is 10 MeV$/c^2$. The uncertainty due to binning is estimated by refitting the data with bin widths of 5, 8 and 12 MeV$/c^2$.

The uncertainty in integrated luminosity is 1.4%. The uncertainties of the intermediate branching fractions are given in Table V. For the $\Upsilon(1S)\eta'[\pi\pi\eta]$ and $\Upsilon(1S)\eta'[\rho\gamma]$ modes, some of the uncertainties cannot be evaluated due to zero signal yield. Such uncertainties are assumed to be equal to those in the $\Upsilon(1S)\eta[3\pi]$ mode. The total uncertainty is evaluated as the quadratic sum from all sources.

V. CROSS-CHECK WITH $\Upsilon(5S) \to \Upsilon(2S)[\Upsilon(1S)\gamma\gamma]\pi^+\pi^-$

To validate the analysis procedure we measure the known process $e^+e^- \to \Upsilon(2S)\pi^+\pi^-$, where $\Upsilon(2S)$ is

TABLE V. Branching fractions used in this work.

Decay	Branching fraction [1] (%)
$\Upsilon(1S) \to \mu^+\mu^-$	2.48 ± 0.05
$\Upsilon(2S) \to \mu^+\mu^-$	1.93 ± 0.17
$\Upsilon(2S) \to \Upsilon(1S)\pi^+\pi^-$	17.85 ± 0.26
$\eta \to \gamma\gamma$	39.41 ± 0.2
$\eta \to \pi^+\pi^-\pi^0$	22.92 ± 0.28
$\eta' \to \pi^+\pi^-\eta$	42.5 ± 0.5
$\eta' \to \rho^0\gamma$	29.5 ± 0.4
$\pi^0 \to \gamma\gamma$	98.823 ± 0.034

reconstructed via the decay chain $\Upsilon(2S) \to \chi_{bJ}(1P)\gamma$, $\chi_{bJ}(1P) \to \Upsilon(1S)\gamma$, $\Upsilon(1S) \to \mu^+\mu^-$, and $J = 0, 1, 2$. The cross section for this process is measured independently with the $\Upsilon(2S) \to \mu^+\mu^-$ decay where the statistics of signal events is much higher [30].

The analysis procedure is almost the same as for the other modes. Selection criteria for this process are based on the same set of common variables: $\Upsilon(1S)$ meson is reconstructed by the $M_{\mu\mu}$ in the $9.235\ \mathrm{GeV}/c^2 < M_{\mu\mu} < 9.685\ \mathrm{GeV}/c^2$ range, the angle $\Psi > 2.6$ radian, and the total reconstructed energy $10.75\ \mathrm{GeV} < E_{\mathrm{tot}} < 10.94\ \mathrm{GeV}$. In addition, a requirement on the mass recoiling off two charged pions, $M^{\mathrm{rec}}_{\pi\pi}$, is applied as $|M^{\mathrm{rec}}_{\pi\pi} - M_{\Upsilon(2S)}| < 30\ \mathrm{MeV}/c^2$. According to MC simulation, the resolution of $M^{\mathrm{rec}}_{\pi\pi}$ is $6\ \mathrm{MeV}/c^2$. This helps to reduce background from the $e^+e^- \to \Upsilon(1D)\pi^+\pi^-$ process, where $\Upsilon(1D) \to \chi_{bJ}\gamma$, $\chi_{bJ}(1P) \to \Upsilon(1S)\gamma$.

Each candidate event contains two $\mu^+\mu^-\gamma$ combinations. The one with the larger value of $M_{\mu\mu\gamma} - M_{\mu\mu}$ is taken to be the candidate for $\chi_{bJ}(1P) \to \Upsilon(1S)\gamma$. The studied process results in peaks at 399.1, 432.5, and 451.9 MeV/c^2 for $J = 0, 1, 2$, respectively. Distributions for each $\chi_{bJ}(1P)$ are fitted to the sum of a Crystal Ball function and a Gaussian in the same way as for the other processes. Reconstruction efficiencies are $\varepsilon_{\chi_{b0}(1P)} = 28.12 \pm 0.04\%$, $\varepsilon_{\chi_{b1}(1P)} = 28.68 \pm 0.04\%$, and $\varepsilon_{\chi_{b2}(1P)} = 28.52 \pm 0.04\%$.

The known products of the intermediate branching fractions $\mathcal{B}_{\chi_{bJ}(1P)} = \mathcal{B}(\Upsilon(2S) \to \chi_{bJ}(1P)\gamma) \times \mathcal{B}(\chi_{bJ}(1P) \to \Upsilon(1S)\gamma)$ are $\mathcal{B}_{\chi_{b0}(1P)} = (7.37 \pm 1.28) \times 10^{-4}$, $\mathcal{B}_{\chi_{b1}(1P)} = (242 \pm 19) \times 10^{-4}$, and $\mathcal{B}_{chib2(1P)} = (128 \pm 9) \times 10^{-4}$ [1]. The relative contributions to the signal, $\varepsilon_{\chi_{bJ}(1P)} \times \mathcal{B}_{\chi_{bJ}(1P)}$, for $J = 0, 1, 2$ are in the ratios $0.029 : 1 : 0.527$. The total MC signal line shape is the sum of three contributions, with all parameters except an overall normalization factor being fixed for the data analysis. The total branching fraction weighted with the efficiency is $\mathcal{B}_{\Upsilon(2S)\pi\pi} = \mathcal{B}(\Upsilon(1S) \to \mu^+\mu^-) \sum \varepsilon_{\chi_{bJ}(1P)} \times \mathcal{B}(\Upsilon(2S) \to \chi_{bJ}(1P)\gamma) \times \mathcal{B}(\chi_{bJ}(1P) \to \Upsilon(1S)\gamma) = (2.69 \pm 0.16) \times 10^{-4}$, and is used to calculate the cross section [Eq. (2)].

Figure 4 shows the experimental $M_{\mu\mu\gamma} - M_{\mu\mu}$ distribution. The signal yield is determined from fitting the $M_{\mu\mu\gamma} - M_{\mu\mu}$ distribution, with the fit function being the sum of the total MC signal line shape and a background function $(x - p_1)^{p_2} e^{p_3 x}$. We obtain $N_{\mathrm{sig}} = 85.32 \pm 11.5$, resulting in the Born cross section $\sigma_{\mathrm{B}}(e^+e^- \to \Upsilon(2S)\pi^+\pi^-) = 3.98 \pm 0.54\,\mathrm{pb}$ (statistical uncertainty only). This value is consistent with the independent measurement $\sigma_{\mathrm{B}}(e^+e^- \to \Upsilon(2S)\pi^+\pi^-) = 4.07 \pm 0.16 \pm 0.45$ pb [30] within the uncertainty.

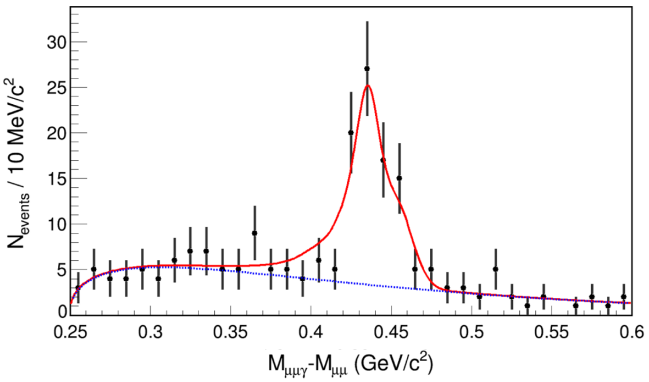

FIG. 4. The $M_{\mu\mu\gamma} - M_{\mu\mu}$ distribution for the $e^+e^- \to \Upsilon(2S)\pi^+\pi^-$ process, where $\Upsilon(2S) \to \chi_{bJ}(1P)\gamma \to \Upsilon(1S)\gamma\gamma \to \mu^+\mu^-\gamma\gamma$. Data are shown as points, the solid red line shows the best fit to the data, and the dashed blue line shows the background contribution.

VI. CONCLUSION

In summary, using the Belle data sample of 118.3 fb^{-1} obtained at $\sqrt{s} = 10.866$ GeV, we report measurements of the cross sections for the processes $e^+e^- \to \Upsilon(1S, 2S)\eta$, and set an upper limit on the cross section of $e^+e^- \to \Upsilon(1S)\eta'$. The measured Born cross sections, with initial-state radiation being taken into account, are [Eq. (3)] $\sigma_{\mathrm{B}}^{\eta\to 3\pi}(e^+e^- \to \Upsilon(2S)\eta) = 2.08 \pm 0.29 \pm 0.20$ pb, $\sigma_{\mathrm{B}}^{\eta\to 2\gamma}(e^+e^- \to \Upsilon(2S)\eta) = 2.07 \pm 0.30 \pm 0.28$ pb, $\sigma_{\mathrm{B}}^{\eta\to 3\pi}(e^+e^- \to \Upsilon(1S)\eta) = 0.42 \pm 0.08 \pm 0.04$ pb, $\sigma_{\mathrm{B}}^{\eta'\to\pi\pi\eta}(e^+e^- \to \Upsilon(1S)\eta') < 0.052$ pb, C.L. $= 90\%$, $\sigma_{\mathrm{B}}^{\eta'\to\rho^0\gamma}(e^+e^- \to \Upsilon(1S)\eta') < 0.053$ pb, C.L. $= 90\%$.

The weighted averages for the corresponding modes are $\sigma_{\mathrm{B}}(e^+e^- \to \Upsilon(2S)\eta) = 2.07 \pm 0.21 \pm 0.19$ pb, $\sigma_{\mathrm{B}}(e^+e^- \to \Upsilon(1S)\eta) = 0.42 \pm 0.08 \pm 0.04$ pb, $\sigma_{\mathrm{B}}(e^+e^- \to \Upsilon(1S)\eta') < 0.037$ pb, C.L. $= 90\%$.

The significances exceed 10σ for $e^+e^- \to \Upsilon(1S)\eta$ and $e^+e^- \to \Upsilon(2S)\eta$, and we claim first observations of these processes. For $e^+e^- \to \Upsilon(2S)\eta$, our measured cross section is statistically consistent with the previous result [12] within $\sim 2.3\sigma$. Such a discrepancy can be accounted for by statistical fluctuation. For $e^+e^- \to \Upsilon(1S)\eta$, our result is consistent with the published result.

Under the assumption that these processes proceed only through the $\Upsilon(5S)$, we calculate branching fractions with the formula $\mathcal{B}(\Upsilon(5S) \to X) = \sigma_{\mathrm{vis}}(e^+e^- \to X)/\sigma(e^+e^- \to \Upsilon(5S))$, where $\sigma_{\mathrm{vis}}(e^+e^- \to \Upsilon(5S)) = 0.340 \pm 0.016$ nb [32]:

$\mathcal{B}(\Upsilon(5S) \to \Upsilon(1S)\eta) = (0.85 \pm 0.15 \pm 0.08) \times 10^{-3}$,
$\mathcal{B}(\Upsilon(5S) \to \Upsilon(2S)\eta) = (4.13 \pm 0.41 \pm 0.37) \times 10^{-3}$,
$\mathcal{B}(\Upsilon(5S) \to \Upsilon(1S)\eta') < 7.3 \times 10^{-5}$, C.L. = 90%.

Using $\sigma(e^+e^- \to \Upsilon(1S)\pi^+\pi^-) = 2.27 \pm 0.12 \pm 0.14$ pb, $\sigma(e^+e^- \to \Upsilon(2S)\pi^+\pi^-) = 4.07 \pm 0.16 \pm 0.45$ pb [30] and the obtained Born cross section, we also calculate the width ratios between η and dipion transitions to be

$$\frac{\Gamma(\Upsilon(5S) \to \Upsilon(1S)\eta)}{\Gamma(\Upsilon(5S) \to \Upsilon(1S)\pi^+\pi^-)} = 0.19 \pm 0.04 \pm 0.01 \quad (4)$$

and

$$\frac{\Gamma(\Upsilon(5S) \to \Upsilon(2S)\eta)}{\Gamma(\Upsilon(5S) \to \Upsilon(2S)\pi^+\pi^-)} = 0.51 \pm 0.06 \pm 0.04, \quad (5)$$

where correlated systematic uncertainties cancel in the ratio. These values are significantly larger than the predicted values of ∼0.03 for $\Upsilon(2S)$ and ∼0.005 for $\Upsilon(1S)$, calculated in the QCDME regime [5], and may be compared to $\frac{\Upsilon(4S)\to\Upsilon(1S)\eta}{\Upsilon(4S)\to\Upsilon(1S)\pi^+\pi^-} = 2.41 \pm 0.40 \pm 0.12$ [8], measured in a regime where QCDME is no longer valid. Similarly, our measured upper limit on the ratio between the η' and η transitions is

$$\frac{\Gamma(\Upsilon(5S) \to \Upsilon(1S)\eta')}{\Gamma(\Upsilon(5S) \to \Upsilon(1S)\eta)} < 0.10 \quad (\text{C.L.} = 90\%), \quad (6)$$

which is significantly smaller than the value ≈12 predicted by the naive QCDME model [2].

As shown in Refs. [2,3], a suggested solution is the existence of a light-flavor admixture to the $b\bar{b}$ state. Such a structure of the $\Upsilon(5S)$ resonance could result in a larger cross section for $e^+e^- \to \Upsilon(1S, 2S)\eta$ and $e^+e^- \to \Upsilon(1S)\eta'$ processes and lead to dominance of the $e^+e^- \to \Upsilon(1S, 2S)\eta$ process over $e^+e^- \to \Upsilon(1S)\eta'$ [3]:

$$\frac{\Gamma(\Upsilon(5S) \to \Upsilon(1S)\eta')}{\Gamma(\Upsilon(5S) \to \Upsilon(1S)\eta)} \approx \frac{p_{\eta'}^3}{2p_\eta^3} = 0.25, \quad (7)$$

still higher than the obtained limit. Such suppression has also been observed in Ref. [33], where $\frac{\Gamma(\Upsilon(4S)\to\Upsilon(1S)\eta')}{\Gamma(\Upsilon(4S)\to\Upsilon(1S)\eta)}$ is reported to be 0.20 ± 0.06, in agreement with the expected value in the case of an admixture of a state containing light quarks.

ACKNOWLEDGMENTS

We thank the KEKB group for the excellent operation of the accelerator; the KEK cryogenics group for the efficient operation of the solenoid; and the KEK computer group, and the Pacific Northwest National Laboratory (PNNL) Environmental Molecular Sciences Laboratory (EMSL) computing group for strong computing support; and the National Institute of Informatics, and Science Information NETwork 5 (SINET5) for valuable network support. We acknowledge support from the Ministry of Education, Culture, Sports, Science, and Technology (MEXT) of Japan, the Japan Society for the Promotion of Science (JSPS), and the Tau-Lepton Physics Research Center of Nagoya University; the Australian Research Council including Grants No. DP180102629, No. DP170102389, No. DP170102204, No. DP150103061, and No. FT130100303; Austrian Federal Ministry of Education, Science and Research (FWF) and FWF Austrian Science Fund No. P 31361-N36; the National Natural Science Foundation of China under Contracts No. 11435013, No. 11475187, No. 11521505, No. 11575017, No. 11675166, and No. 11705209; Key Research Program of Frontier Sciences, Chinese Academy of Sciences (CAS), Grant No. QYZDJ-SSW-SLH011; the CAS Center for Excellence in Particle Physics (CCEPP); the Shanghai Science and Technology Committee (STCSM) under Grant No. 19ZR1403000; the Ministry of Education, Youth and Sports of the Czech Republic under Contract No. LTT17020; Horizon 2020 ERC Advanced Grant No. 884719 and ERC Starting Grant No. 947006 "InterLeptons" (European Union); the Carl Zeiss Foundation, the Deutsche Forschungsgemeinschaft, the Excellence Cluster Universe, and the VolkswagenStiftung; the Department of Atomic Energy (Project Identification No. RTI 4002) and the Department of Science and Technology of India; the Istituto Nazionale di Fisica Nucleare of Italy; National Research Foundation (NRF) of Korea Grants No. 2016R1D1A1B01010135, No. 2016R1D1A1B02012900, No. 2018R1A2B3003643, No. 2018R1A6A1A06024970, No. 2019K1A3A7A09033840, No. 2019R1I1A3A01058933, No. 2021R1A6A1A03043957, No. 2021R1F1A1060423, and No. 2021R1F1A1064008; Radiation Science Research Institute, Foreign Large-size Research Facility Application Supporting project, the Global Science Experimental Data Hub Center of the Korea Institute of Science and Technology Information and KREONET/GLORIAD; the Polish Ministry of Science and Higher Education and the National Science Center; the Ministry of Science and Higher Education of the Russian Federation, Agreement No. 14.W03.31.0026, and the HSE University Basic Research Program, Moscow; University of Tabuk Research Grants No. S-1440-0321, No. S-0256-1438, and No. S-0280-1439 (Saudi Arabia); the Slovenian Research Agency Grants No. J1-9124 and No. P1-0135; Ikerbasque, Basque Foundation for Science, Spain; the Swiss National Science Foundation; the Ministry of Education and the Ministry of Science and Technology of Taiwan; and the United States Department of Energy and the National Science Foundation.

[1] P. A. Zyla *et al.* (Particle Data Group), Prog. Theor. Exp. Phys. **2020**, 083C01 (2020).
[2] M. B. Voloshin, Mod. Phys. Lett. A **26**, 773 (2011).
[3] M. B. Voloshin, Phys. Rev. D **85**, 034024 (2012).
[4] I. Adachi *et al.* (Belle Collaboration), Phys. Rev. Lett. **108**, 032001 (2012).
[5] M. B. Voloshin and V. I. Zakharov, Phys. Rev. Lett. **45**, 688 (1980).
[6] A. Bondar *et al.* (Belle Collaboration), Phys. Rev. Lett. **108**, 122001 (2012).
[7] M. B. Voloshin, Prog. Part. Nucl. Phys. **61**, 455 (2008).
[8] B. Aubert *et al.* (*BABAR* Collaboration), Phys. Rev. D **78**, 112002 (2008).
[9] U. Tamponi *et al.* (Belle Collaboration), Phys. Rev. Lett. **115**, 142001 (2015).
[10] F.-K. Guo, C. Hanhart, and Ulf.-G. Meissner, Phys. Rev. Lett. **105**, 162001 (2010).
[11] J. Lees *et al.* (*BABAR* Collaboration), Phys. Rev. D **84**, 092003 (2011).
[12] U. Tamponi *et al.* (Belle Collaboration), Eur. Phys. J. C **78**, 633 (2018).
[13] A. Abashian *et al.* (Belle Collaboration), Nucl. Instrum. Methods Phys. Res., Sect. A **479**, 117 (2002).
[14] J. Brodzicka *et al.* (Belle Collaboration), Prog. Theor. Exp. Phys. **2012**, 04D001 (2012).
[15] S. Kurokawa and E. Kikutani, Nucl. Instrum. Methods Phys. Res., Sect. A **499**, 1 (2003).
[16] T. Abe *et al.*, Prog. Theor. Exp. Phys. **2013**, 03A001 (2013).
[17] D. J. Lange, Nucl. Instrum. Methods Phys. Res., Sect. A **462**, 152 (2001).
[18] R. Brun *et al.*, GEANT 3.21, CERN Report No. DD/EE/84-1, 1984.
[19] J. P. Alexander *et al.* (CLEO Collaboration), Phys. Rev. D **58**, 052004 (1998).
[20] F. Ambrosino *et al.* (KLOE Collaboration), J. High Energy Phys. 05 (2008) 006.
[21] N. Davidson, T. Przedzinski, and Z. Was, Comput. Phys. Commun. **199**, 86 (2016).
[22] A. Abashian *et al.*, Nucl. Instrum. Methods Phys. Res., Sect. A **491**, 69 (2002).
[23] K. Hanagaki, H. Kakuno, H. Ikeda, T. Iijima, and T. Tsukamoto, Nucl. Instrum. Methods Phys. Res., Sect. A **485**, 490 (2002).
[24] T. Skwarnicki, Ph.D. thesis, Cracow, INP, 1986.
[25] D. Santel *et al.* (Belle Collaboration), Phys. Rev. D **93**, 011101 (2016).
[26] R. Mizuk *et al.* (Belle Collaboration), J. High Energy Phys. 10 (2019) 220.
[27] R. Mizuk *et al.* (Belle Collaboration), Phys. Rev. Lett. **117**, 142001 (2016).
[28] M. Benayoun, S. Eidelman, V. Ivanchenko, and Z. Silagadze, Mod. Phys. Lett. A **14**, 2605 (1999).
[29] S. Actis *et al.* (Working Group on Radiative Corrections, Monte Carlo Generators for Low Energies), Eur. Phys. J. C **66**, 585 (2010).
[30] A. Garmash *et al.* (Belle Collaboration), Phys. Rev. D **91**, 072003 (2015).
[31] M. Ablikim *et al.* (BESIII Collaboration), Phys. Rev. D **83**, 012003 (2011).
[32] S. Esen *et al.* (Belle Collaboration), Phys. Rev. D **87**, 031101 (2013).
[33] E. Guido *et al.* (Belle Collaboration), Phys. Rev. Lett. **121**, 062001 (2018).